DOI: 10.21857/y26kecd7x9

Pregledni članak / Review paper
Prihvaćeno / Accepted: 15. svibnja 2025.

SURFACE ELECTROMAGNETICS: DEVELOPMENT, MODELING AND APPLICATIONS

Zvonimir Šipuš, Marko Bosiljevac and Davorin Mikulić

Abstract

Ideal boundary conditions are widely used in most electromagnetic solvers to approximate the behavior of actual surfaces or materials. For example, it is common to replace metal conductors with perfect electric conductors (PECs), thus greatly simplifying computational requirements. Perfect magnetic conductor (PMC) boundary condition is also often used in the first stage of electromagnetic simulations, even though magnetic conductors at microwave frequencies do not exist in nature. The reason is that some artificial surfaces exhibit magnetic conducting properties in certain frequency bands. Furthermore, many other artificial surface types, in addition to the ones mentioned above, have emerged over the recent years, and are commonly used in various applications. This paper provides an overview of surface electromagnetics, a broad concept that refers to a wide range of electromagnetic surfaces, beginning with the simplest canonical uniform surfaces and progressing to more complex structures. It explores the development and applications of canonical electromagnetic surfaces for microwave applications, demonstrating their ability to enhance guiding and radiation properties. This includes in particular the coupling between different parts of the considered component and the control of antenna radiation properties, such as beam direction, beamwidth, sidelobe level and polarization. The paper further discusses theoretical models that can be used in the initial stage of the design in which the considered structure is modelled using canonical EM surfaces. Surface electromagnetics has been shown to be a versatile, robust, and cost-effective solution for the design of the next-generation EM components, allowing full customization of component properties.

Keywords: surface electromagnetics; canonical electromagnetics surfaces; soft surfaces; hard surfaces; electromagnetic band-gap structures; gap-waveguide technology; metasurfaces; transverse resonant method; equivalence principle; microwave holograms.

1 Introduction

When designing electromagnetic components, the first step is most often related to the conceptual design, that is, contemplating how we would like EM waves to travel along the structure or interact with it in order to produce the desired effect. Thin structures or surfaces are often used to direct EM waves, and this is why research field called surface electromagnetics has developed, and has become one the most impactful in the EM community in the recent years. Applications of this research today span the use of reconfigurable intelligent surfaces in mobile communication systems to custom built reflective metasurfaces used on satellites for selective coverage of the Earth. However, before starting with the actual complex design for a specific application, which is usually done by means of general EM solver and suitable optimization routine, it is crucial to make a simplified design, where the focus is on basic EM phenomena that enable the construction of considered EM components. Therefore, canonical EM surfaces with different levels of complexity, enabling different phenomena, are the basis of understanding and implementing the surface electromagnetics.

Historically, the attempts to control the propagation of EM waves using innovative surfaces were first proposed in 19th century by Lamb, who investigated the reflection and transmission from an array of metallic strips [1]. Based on this idea, Marconi used arrays of parallel wires to obtain reflectors for one polarization only [2]. Another example is related to the concept of the Fresnel lens demonstrated approximately 150 years before the use in radio transmitters [3], [4]. All these structures actually contain surfaces that can be described with spatially-varying or polarization-dependent boundary conditions. Starting from the basic surfaces such as PEC and PMC, researchers have developed different concepts of developing and applying these surfaces, for example, the control of surface waves through surface parameter modulation [5], transmissive or reflective surfaces for frequency control known as frequency selective surfaces (FSS) [6], electromagnetic bandgap surfaces (EBG) for coupling control and realization of low-profile antennas [7], and the development of metasurfaces through integration with metamaterial concepts [8].

The goal of this review paper is to explain different EM surface concepts and typical structures for their realization. We will start with essential canonical surfaces, the well-known perfect electric conductor (PEC) and perfect magnetic conductor (PMC); based on the properties of waves propagating along such surfaces, the new canonical surfaces will be revealed as a natural evolution from this basis. These are soft and hard surfaces, and their two-dimensional generalization electromagnetic band-gap (EBG) structures. Additionally, starting from the realization of waveguide structures and me-

tamaterials, we will also focus on the gap-waveguide concept and metasurfaces. These canonical surfaces offered new technological ideas in the production of electromagnetic components, of particular interest in mm-wave and sub-THz frequency range, where the physical dimensions start to be small since they are related to the wavelength (1 cm at 30 GHz or 1 mm at 300 GHz). Developed technology, in turn, allows presently the construction of EM components with properties that were not possible to achieve using traditional technology. Furthermore, some of these structures enable the physical realization of concepts, such as equivalence principle, that were previously used only in the mathematical modelling of various EM problems. Therefore, the goal of the paper is to give an overview of ideas and realizations that are part of surface electromagnetics and that have been intensively investigated over the last 30 years.

2 Canonical electromagnetic surfaces

The most commonly used canonical surface is undoubtedly the perfect electric conductor (PEC). In microwave frequency range, there are several types of conductors with good conductivity, which are therefore often approximated as PEC (with high accuracy). The boundary conditions, which are used to describe PEC, are defined with the tangential components of the electric field which are ideally equal to zero, i.e., $\mathbf{E}_{\mathbf{tan}} = 0$. It should be noted that there is no simple equation for the tangential magnetic field, i.e., the discontinuity in the tangential magnetic field just above the PEC surface and within the PEC structure is described by the surface current $\mathbf{J} = \hat{n} \times \mathbf{H}$, where $\hat{n}$ is the unit vector normal to the PEC surface.

Although looking at these boundary conditions everything seems quite trivial, if we look at EM waves propagating along the PEC surface, we come to an important difference regarding the propagation of waves with different characteristic polarizations. A wave with the electric field parallel to the PEC surface (the so-called parallel polarization, $\mathbf{E}_{\mathrm{HOR}}$ in Figure 1.) cannot propagate along a PEC surface simply because the boundary condition $\mathbf{E}_{\mathrm{tan}} = 0$ does not allow it. Therefore, we can say that the PEC surface has the STOP property for parallel polarization. However, a wave with perpendicular polarization (i.e., with electric field perpendicular to the PEC surface, $\mathbf{E}_{\mathrm{VER}}$ in Figure 1.) has the GO property, i.e., the PEC surface supports the propagation of perpendicularly polarized waves along the PEC surface.

The next canonical surface is a perfect magnetic conductor (PMC). Since Maxwell's equations support duality property, the PMC surface can be described as a dual to the PEC surface. In other words, the boundary condition describing the PMC is $\mathbf{H}_{\mathrm{tan}} = 0$. Thus, waves propagating along the PMC surface have a dual property: perpendicular

polarization waves cannot propagate along the PMC surface (because the magnetic field is tangential to the PMC surface), i.e., they have the STOP property, while parallel polarization waves propagate unhindered along the PMC surface (i.e., they have the GO property). It should be noted that in the microwave frequency range, there is no material that would be accurately approximated with the PMC boundary condition; however, there are structures that successfully replace PMC surfaces, as will be demonstrated shortly.

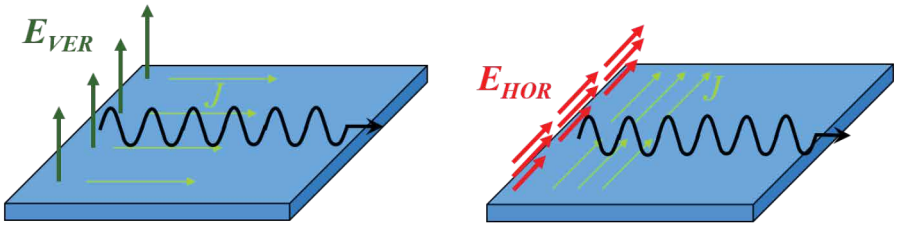

Figure 1. Sketch of the EM problem under consideration – EM wave propagating along a generic surface (both principal polarizations are sketched).

Table 1. Characteristics of different types of canonical EM surfaces

Canonical Surface	E-field Polarization	
	VER or TM	HOR or TE
PEC	GO	STOP
PMC	STOP	GO
PEC/PMC strip grid - SOFT	STOP	STOP
PEC/PMC strip grid - HARD	GO	GO
EBG - Grazing	STOP	STOP
EBG (PMC type) - Close to normal	PMC	

The STOP and GO property of PEC and PMC surfaces for two principal polarizations is given in Table 1 (according to [9]).

We do not often have a wave of only one principle polarization present, that is, we have a more complex "mixed" case. Therefore, the question arises whether there is a canonical surface that would have the STOP or GO property for both polarizations. Such surfaces were described by P.-S. Kildal in the late 1980s; they were called soft and hard surfaces [10], [11]. In their most basic canonical form, such surfaces consist of PEC/PMC parallel stripes, as shown in Figure 2. In this way, an anisotropic structure is obtained; therefore, the properties of EM waves propagating along the structure depend on the direction of propagation. If the wave propagates perpendicular to the PEC/PMC, we obtain the STOP property for both polarizations: the wave with parallel polarization stops at the electric stripes (because $\mathbf{E}_{tan} = 0$ on them), while the wave with perpendicular polarization stops at the magnetic stripes (because $\mathbf{H}_{tan} = 0$ there). On the contrary, the wave propagating along the stripes propagates unhindered (not-obstructed), and thus we obtain the GO property. The dispersion properties of the PEC/PMC structure have been rigorously analyzed in [12], [13], confirming this intuitive approach in describing their properties.

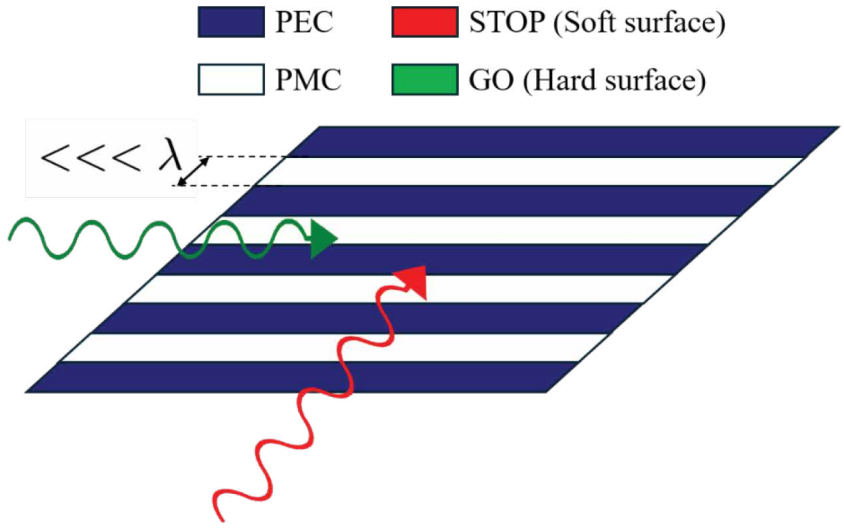

Figure 2. Construction of soft and hard EM surfaces

With the theoretical concept in place, the question of the practical realization of PEC/PMC canonical surface arises since there is no material that would successfully "imitate" the PMC surface in the microwave frequency range. Fortunately, the basic the-

ory of transmission lines states that a transmission line of a quarter-wavelength length transforms a load of zero impedance (i.e., the PEC surface) into a load of infinite impedance (i.e., the PMC surface). This is achieved by stacking a series of vertically oriented parallel-plate waveguides (PPW) used as transmission lines, as shown in Figure 3. The result is a corrugated structure with a corrugation depth of a quarter wavelength. and it represents a practical realization of the PEC/PMC canonical surface in soft direction. In hard direction, the condition is somewhat different, i.e., the depth of corrugations h_{corr} needed to obtain the hard surface is $h_{corr} = \lambda_0 / 4\sqrt{\varepsilon_r - 1}$ (consequently, the corrugations should be filled with dielectric in order to obtain the hard boundary condition).

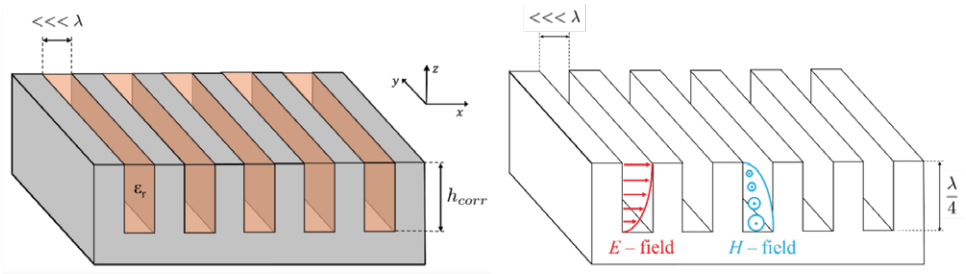

(a) (b)

Figure 3. (a) Geometry of the corrugated surface – realization of soft and hard surfaces; (b) E- and H-field distribution in λ/4 thick transverse corrugations.

After describing one realization of soft and hard surfaces, practical questions arise: are corrugations soft surfaces only at one frequency (i.e., in a narrow range around that frequency) or can we use corrugated surfaces to create structures with a wider frequency bandwidth? As will be shown in the next chapter, the bandwidth of corrugated soft surfaces is 2:1, which is considered a significant bandwidth in the microwave frequency range. The next question is whether it is possible to create a structure thinner than a quarter wavelength (this can be a significant thickness at lower frequencies). Again, this can be done in two ways – either by filling the corrugations with a dielectric that reduces the wavelength, thus the thickness of the corrugations; or by changing the topology of the corrugations according to Figure 4.a. The topology in Figure 4.a can further be modified into a low-cost realization of soft and hard surfaces using printed circuit board (PCB) technology. This is possible by using strips grounded by vias (as shown

in Figure 4.b.). However, one should note that the bandwidth of such modified surfaces will be smaller [14]).

As an illustrative example of using soft surfaces, let us consider a monopole antenna with a corrugated ground plane. In a classic example case, the ground plane is simply a conductor plate usually made of copper (as illustrated in Figure 5.a). However, due to the finite size of the ground plane, vertically-polarized EM waves (excited by a monopole antenna) will diffract at the ground plane edges, causing perturbations in the radiation pattern, usually in a non-controllable way. Due to this, there is a requirement to suppress the diffracted fields from the edges, as well as backside radiation, which can easily be obtained by using rotationally-symmetric corrugated ground plane (Figure 5.b). Now the radiation pattern resembles the one of the ideal antenna, with suppressed backside radiation (see [16] – [18] for details).

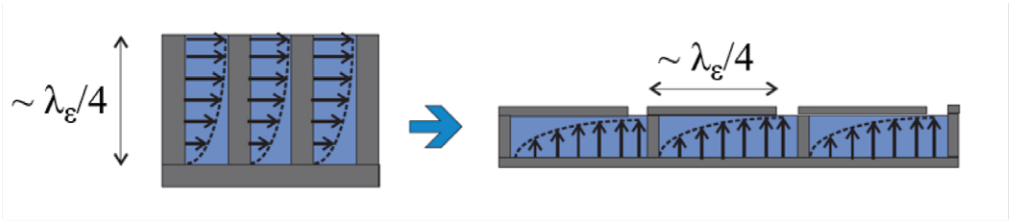

(a)

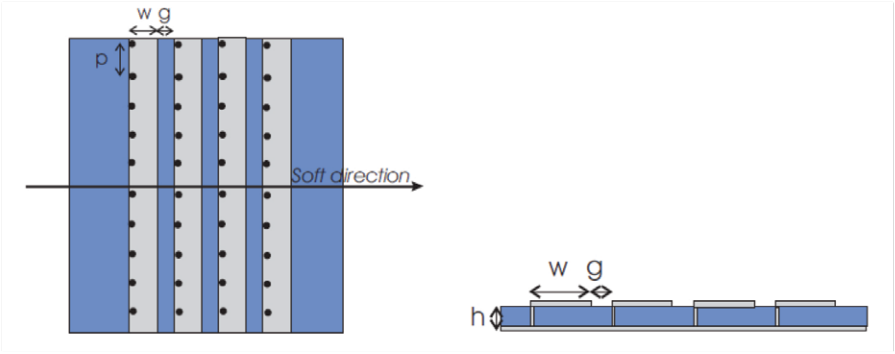

(b)

Figure 4. (a) Thickness reduction of corrugated surfaces,
(b) PCB realization of corrugated surfaces (according to [15])

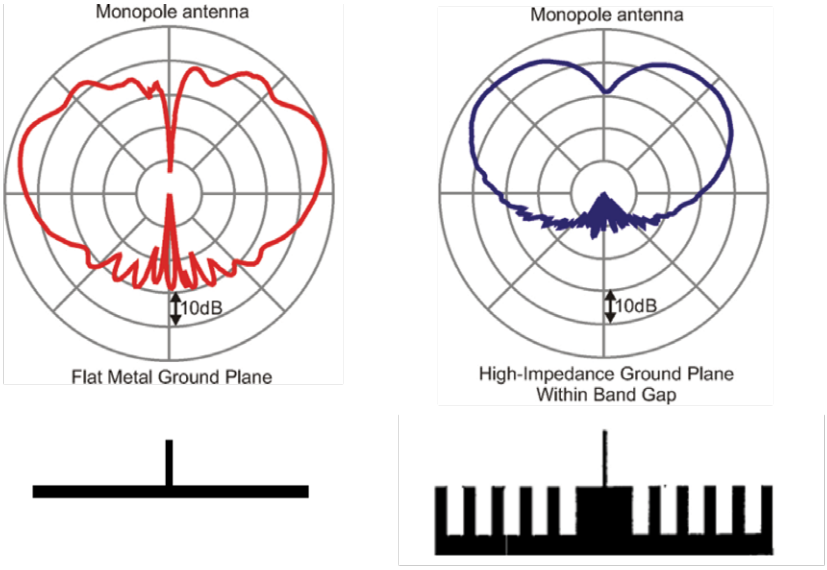

(a) (b)

Figure 5. Comparison of radiation patterns of a monopole antenna with a flat metal (a) and corrugated ground plane (b). Both considered structures are rotationally symmetric (according to [16] and [18]).

As an example of using hard surfaces, let us consider a transverse electro-magnetic (TEM) waveguide. In classical metallic waveguides (with rectangular or circular cross-section), it is not possible to obtain TEM waves due to boundary condition at the metallic walls, namely where tangential electric field should be zero. Therefore, for the dominant mode, the classical rectangular waveguide can be considered a waveguide with two hard and two soft surfaces. In order to obtain TEM wave, all walls should be hard, i.e., this can be obtained using two PEC and two PMC walls (the PMC walls in this case can be obtained in various ways, the simplest one is to use dielectric slabs attached to the lateral waveguide walls of thickness $h_{die} = \lambda_0 / 4\sqrt{\varepsilon_r - 1}$, see Figure 6 and [19] - [21]).

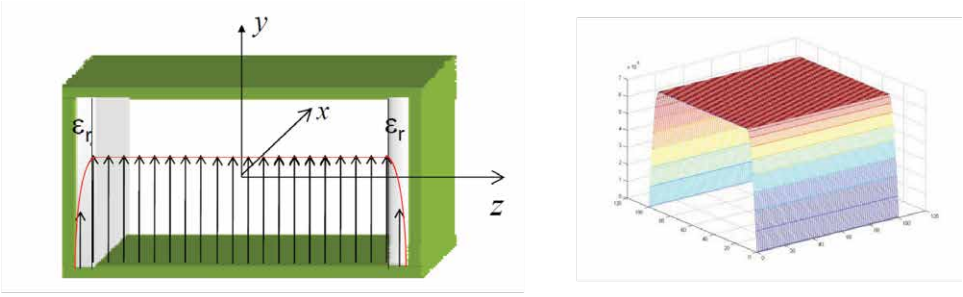

(a) (b)

Figure 6. (a) TEM rectangular waveguide realized with dielectric slabs attached to the lateral walls, and (b) Distribution of the E-field in the waveguide at the hard frequency defined with $\lambda_0 = 4h_{die}\sqrt{\varepsilon_r - 1}$ (according to [22]).

Electromagnetic band-gap structures

The introduced soft surfaces are anisotropic, i.e., they have "ideal" STOP property in only one direction, but also exhibit this property in a relatively wide angular range. However, the natural question is whether it is possible to realize an isotropic soft surface with STOP property in all directions. In 1999, a new type of EM surfaces has been introduced – the electromagnetic bandgap structures (EBGs) and its typical representative – the mushroom structure, see Fig. 7 [18]. By looking at its cross-section, one can consider it as a two-dimensional version of corrugations realized using PCB technology (as shown in Fig. 4.b). The obtained dispersion diagrams show that mushroom structure exhibits STOP property in all directions, but in a smaller frequency band. Furthermore, if we consider the reflections of waves propagating normal to the EBG surface, one can realize that the phase of the reflected wave is around zero (the amplitude is naturally equal to one), which means that such a structure is actually a realization of a PMC. Therefore, EBG structures are interesting from two aspects – creating STOP property for EM waves with grazing incidence, and an artificial magnetic conductor (AMC) for EM waves with approximately normal incidence.

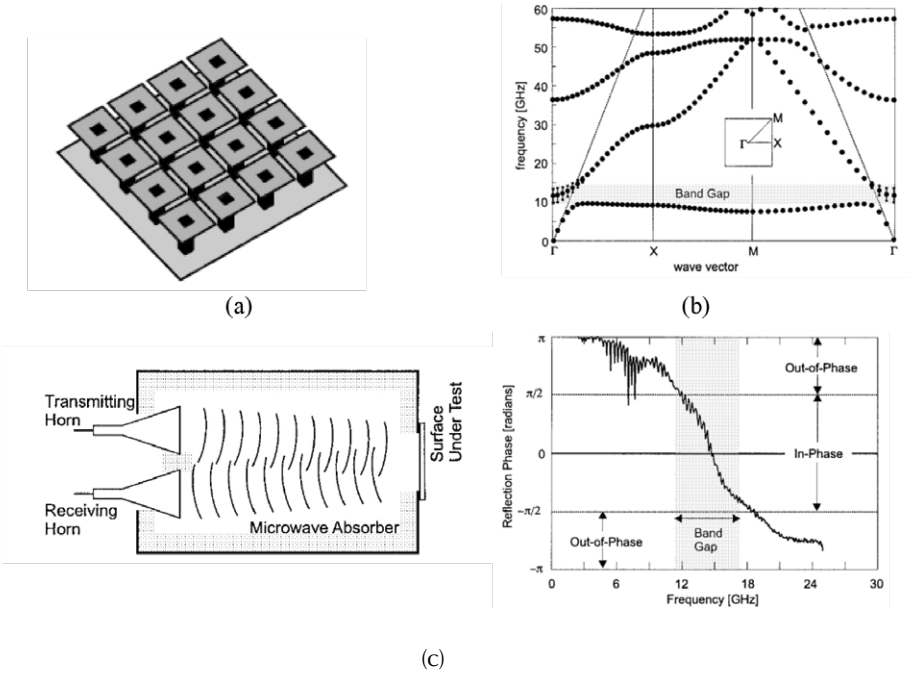

Figure 7. (a) Sketch of the mushroom structure; (b) Dispersion diagram of mushroom structure with indicated band-gap; (c) Measurement of phase of reflection coefficient for nearly normal incidence (reprinted from [18]).

As illustration, let us consider a curl antenna over an EBG ground plane [23] (Figure 8.a). Since the height of the antenna above the ground plane is only 3 mm, the curl over the PEC ground plane has very poor radiating properties (related to both impedance matching and the obtained main beam E-field magnitude). In contrast, the curl over the EBG ground plane shows improved radiating properties in the frequency range from 6 GHz to 8.5 GHz due to the in-phase reflection feature of the EBG ground plane.

The second example (in Figure 8.b) is related to a two-patch array separated in the E-plane [24]. Since the E-plane coupled microstrip antenna array on a thick and high permittivity substrate suffers from strong mutual coupling, the coupling reduction was necessary; it was achieved by inserting an EBG structure between the patches. In other words, the capability of EBG structure to suppress surface waves is used in the array design. Note that four rows of EBG cells are used here to obtain a satisfactory result (reduction of mutual coupling by 8 dB).

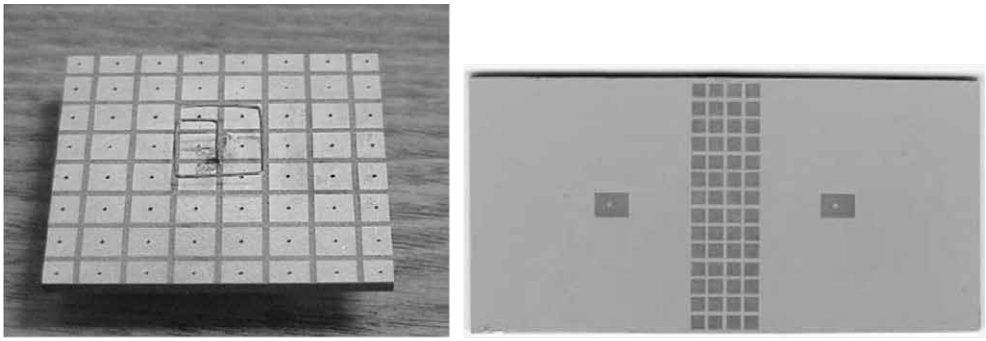

Figure 8. A photograph of a low profile curl antenna (a) and of a microstrip antenna arrays with the EBG structure for mutual coupling reduction (b). Pictures are reprinted from [23] and [24], respectively.

Mathematical description and method of analysis

The properties of canonical surfaces can be investigated in various ways. The first step in the analysis and design procedure is calculating the dispersion diagram that gives information about how the EM waves propagate along the considered surface (regardless of the analysis method chosen). The approach that is simple to implement and understand is the so-called transverse resonant method [25]. If we consider an EM surface without losses, there is possibility of propagation of waves that are trapped to the surface boundary and do not radiate into the space above the surface. The way how these modes are determined resembles the way how the microwave oscillators are analyzed – the sum of surface impedances looking upward and downward should be zero:

$$Z^{(\mathrm{up})} + Z^{(\mathrm{down})} = 0 \tag{1}$$

In other words, for each frequency of interest, we are searching for the propagation constant that fulfils eq. (1). If such propagation constant does not exist, the considered frequency is in the bandgap, i.e., the waves cannot propagate along the surface and the STOP property s obtained.

As an example, let us consider the corrugated surface (Fig. 3) and the EM wave propagating in some general direction along the surface (i.e., both k_x and k_y components of the propagation constant are different from zero; here $k_0 = 2\pi/\lambda_0$ is the free-space wave number). If we consider one corrugation as a vertical parallel plate waveguide,

according to the classical transmission line theory, the short circuit at the bottom of corrugations (i.e., zero surface impedance) is transformed into the following surface impedance

$$\frac{E_x^{\text{corr}}}{H_y^{\text{corr}}} = -j\sqrt{\frac{\mu_0}{\varepsilon_0}}\frac{k_0}{\sqrt{\varepsilon_r k_0^2 - k_y^2}}\tan\left(h_{\text{corr}}\sqrt{\varepsilon_r k_0^2 - k_y^2}\right) \tag{2}$$

Let us focus on the waves propagating normal to the corrugations. i.e., let us consider transverse corrugations. The polarization of interest is the vertical (TM) one, for which corrugations act as impedance transformer. The surface impedance of the free-space for TM polarized-waves is equal

$$Z_2^{TM} = \frac{\eta_0 k_{z,2}}{k_0}, \tag{3}$$

where η_0 is the free-space characteristic impedance $\eta_0 = \sqrt{\mu_0/\varepsilon_0}$ and $k_{z,2}$ is the z-component of the propagation constant in air. Since the waves are bounded to the surface interface, they do not radiate into half-space above the surface, and we have exponentially-attenuating evanescent waves in the direction normal to the surface, i.e., $k_{z,2} = -j\alpha_{z,2}$. In other words, free space is capacitive for TM evanescent waves, and the surface impedance should be inductive in order to have wave propagating along the surface.

Using the equations (1)-(3), one obtains the characteristic equation for transverse corrugations

$$\begin{aligned} &Z^{\text{corr}} = -Z_2^{TM} \\ &j\frac{w}{P}\eta_0\frac{1}{k_0\sqrt{\varepsilon_r}}\tan\left(h_{\text{corr}}k_0\sqrt{\varepsilon_r}\right) = j\eta_0\frac{\alpha_{z,2}}{k_0} \end{aligned} \tag{4}$$

Here the factor w/P is approximatively taking into account that the surface is actually an average of PEC (teeth of the corrugations) and of short-circuited PPW. By examining equation (4), one concludes that for the depth of corrugations $\lambda/4 < d < \lambda/2$, the surface impedance of corrugations is capacitive, i.e., the dispersion equation (1) is in the stop-band, and the waves cannot propagate normal to corrugations.

The frequency that defines the hard surface is determined by considering the TEM wave propagating along the corrugations – the required propagation constant is $k_y = k_0$ (i.e., the free-space propagation constant) and longitudinal EM field components are required to be zero. The propagating mode inside (narrow) corrugations is TE_y mode with E_y, H_x and H_z components present (the coordinate system is given in Fig. 3). The propagation constant in z-direction within the corrugations is equal $\sqrt{k_0^2\varepsilon_r - k_y^2}$, and in order to

obtain longitudinal component of magnetic field equal to zero, the phase shift between bottom and top of corrugations should be π/2. The resulting hard frequency condition is

$$h_{\text{corr}}\sqrt{k_0^2\varepsilon_r - k_0^2} = \frac{\pi}{2} \qquad \text{or} \qquad h_{\text{corr}} = \frac{\lambda_0}{4\sqrt{\varepsilon_r - 1}}. \tag{5}$$

3 Gap waveguide technology

The STOP and GO concept has inspired the development of new technologies for the realization of various electromagnetic components, in particular in mm-wave frequency range. A lot of applications have moved to higher frequencies, mostly due to the occupation of lower frequency bands and to the ultimate request for higher data transmission speeds (i.e., the 5G communication systems have moved part of the used spectrum to mm-waves in order to enable wide bandwidth, low-latency data transmission at speeds that exceed 1 Gbps). However, the practical realization of mm-wave components has a lot of challenges, mostly due to higher losses both in dielectric and metallic patterns. For example, if one wishes to realize a bit more complex component in waveguide technology (note that waveguide technology has the lowest losses in comparison to other technologies suitable for production of mm-wave components), then it will be traditionally made from two plates containing the desired pattern, as illustrated in Fig. 9.a. In order to avoid cracks and gaps responsible for a serious leakage of energy in an undesired direction, one should use numerous screws in order to ensure good contact between two plates, which can become very unpractical (see Fig. 9.b). Therefore, there was a quest for new technologies that will simplify the production of mm-wave technologies.

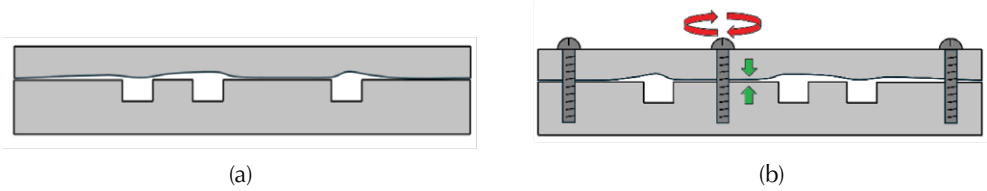

(a) (b)

Figure 9. (a) Sketch of the waveguide component realized from two plates with a gap between the plates; (b) Practical realization of a waveguide component with screws used to avoid gaps and cracks between the plates.

In 2009, a new technology called the gap-waveguide technology was proposed by P.-S. Kildal [26], [27], as a generalization of a waveguide containing corrugated surface as one wall [28], [29]. The basic idea is to replace the lateral walls of waveguide components with a periodic structure that exhibits a band-gap in the operating frequency range. In other words, due to the STOP property of the periodic structure, there is no need for lateral waveguide walls or for tight connections secured with numerous screws between metallic parts forming a waveguide component. One should note that the STOP property is now related to modes propagating within a parallel-plate waveguide, not along an open structure as in the previous examples.

The idea behind this lies in the fact that in parallel-plate waveguide having one PEC wall and one PMC wall, there is no wave propagation if the thickness of such waveguide is smaller than a quarter of the wavelength, see Figure 10. In order to ensure controlled wave propagation in this part of the waveguide (i.e., in order to form a transmission line), a PEC strip is set to be part of the otherwise PMC wall (as shown in Fig. 10.).

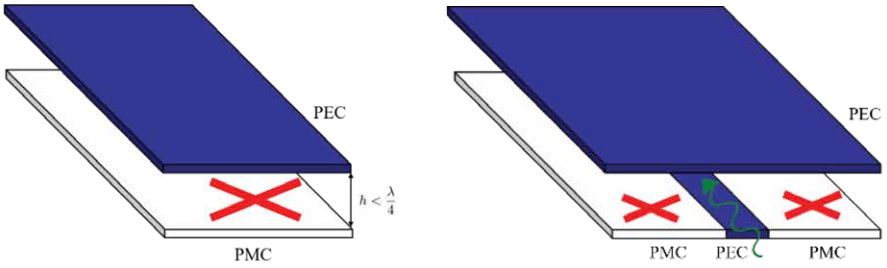

Figure 10. The gap waveguide concept.

As a periodic structure, it has been proposed to implement a two-dimensional array of metallic pins, usually with a square cross-section (the so-called bed-of-nails), see Fig. 11. Since this periodic structure is in the band gap, additional special structure should be introduced to guide the EM waves in the desired direction, and for that either a ridge or groove (Figs. 11.a and 11.b) inside the parallel-plate waveguide is used (the PCB realization is also shown in Figs. 11.c and 11.d). Therewith, the transmission line losses (the basic parameter in selecting the technology in mm-wave and sub-THz frequency bands) are kept at low level, smaller than substrate–integrated waveguide (SIW) or microstrip line technology (more precisely, more than three times and ten times smaller transmi-

ssion losses, respectively). The frequency band in which such a structure can be used in stop band is typically larger than 2:1, which is more than enough for most waveguide components. Table 2 offers a comparison of losses for various transmission lines in mm-wave frequency range [30].

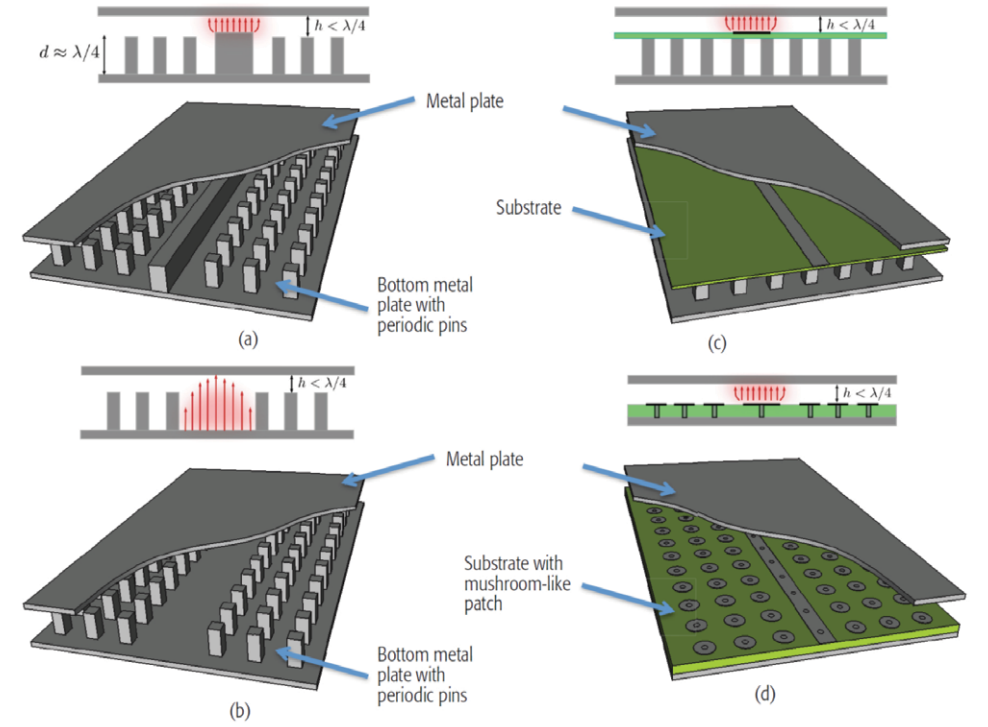

Figure 11. Different realizations of transmission line embedded into the bed-of-nails structure: (a) Ridge, (b) Groove, (c) Inverted microstrip, (d) Microstrip ridge (reprinted from [30]).

Table 2. Losses for different versions of gap waveguides in 60 GHz frequency band

Prototype (frequency)	Simulated loss (dB/cm)	Measured min-max loss (dB/cm)
Rectangular waveguide (50 -75 GHz)	0.0136	0.0295 - 0.042
Groove gap (50 - 75 GHz)	0.019	0.03 - 0.0442
Ridge gap (50 - 75 GHz)	0.0373	0.058 - 0.0705
Microstrip-ridge gap (56 - 68 GHz)	0.0805	0.162 - 0.23
Invert-micro gap (56 - 72 GHz)	0.0934	0.21 -0 .288
Microstrip line (50 - 75 GHz) 0.127 - 0.2 mm substrate	LCP: 0.23	0.62 - 0.77
Microstrip line (50 - 75 GHz) 0.127 - 0.2 mm substrate	Rogers 4003: 0.271	0.7055
Air-filled SIW (50 GHz)	0.0621	0.0615
Rogers-5880, SIW (50 GHz)	0.1327	0.2172

Various components have been realized in gap-waveguide technology, mostly in mm-wave frequency band, such as automotive radar arrays, phased arrays for 5G communication systems, and contact-free waveguide flange adapters for rapid connection of different waveguide components [31] – [35]. Furthermore, the technology is successfully used for packaging of mm-wave components, by which the resonances associated with metallic boxes used for packaging are avoided [36] – [38]. An example how the introduced concepts of various EM structures can be applied in the design of EM devices is illustrated in Fig. 12. The goal was to design a leaky-wave antenna by introducing controlled leakage from one wall of a waveguide transmission line. Therefore, the waveguide is realized using the gap-waveguide technology having three rows of pins on the one side (almost no leakage of energy), and only one row on the other (the ratio of leakage can be controlled by the height of the pins and by the width of the waveguide). Additionally, to prevent the radiation in undesired direction from the radiating aperture, the corrugations are implemented outside, on the top and bottom walls of the parallel-plate waveguide. More details about this antenna design can be found in [39].

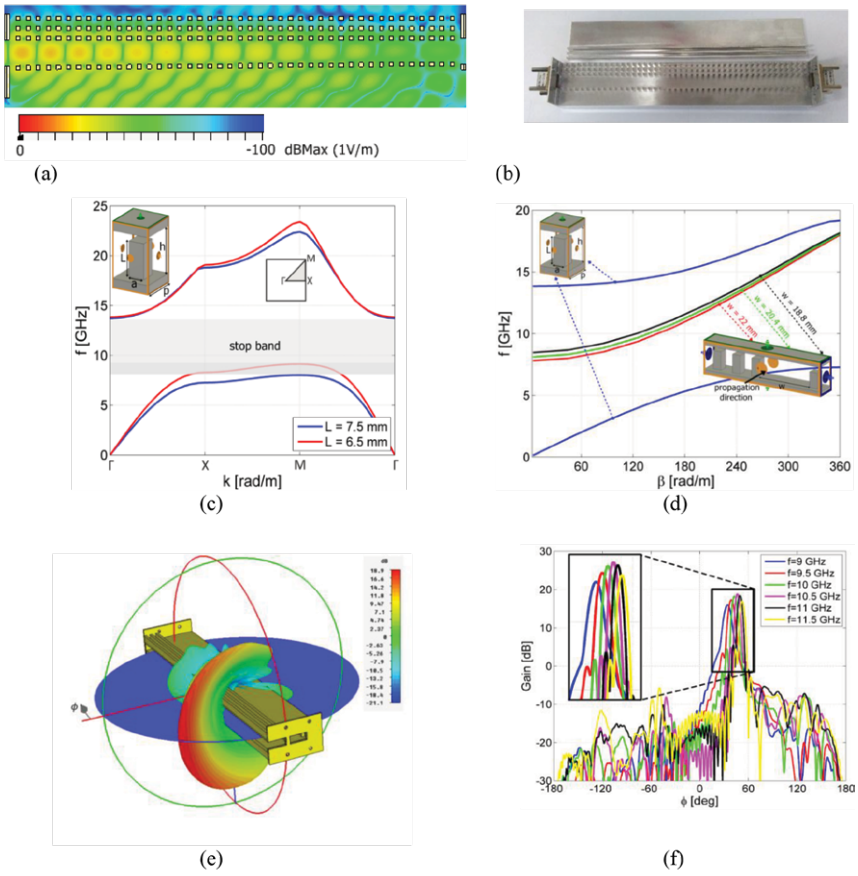

Figure 12. (a) Picture of the gap waveguide leaky wave prototype; (b) E-field distribution of the leaky antenna at 9.5 GHz; (c) Dispersion diagram of a periodic pin unit cell; (d) Dispersion diagram of the groove gap waveguide unit cell; (e) Calculated far-field radiation pattern at 10 GHz; (f) Measured radiation patterns in frequency range of interest (9–11.5 GHz). Reprinted from [39].

More recently, in 2016, a new version of gap-waveguide technology was introduced based on drilling holes in waveguide walls (see Fig. 13). The holes should follow the so-called glide symmetry, i.e., a higher symmetry that combines the translation symmetry for half of the period, and the mirror symmetry through the plane in the middle of the structure [40], [41]. The easiest way to imagine the glide symmetry concept is to look at people's footprints as they walk, for example, in the sand (as sketched in Fig. 13.a). Two properties can then be obtained – either a bandgap with typically 2:1 stopband [42], [43] or a non-dispersive guiding structure related to the first propagating mode

(below the first stopband) [44], [45]. Compared to the technology based on pins, the size of the holes is typically larger than the size of pins (which can be advantageous in a higher part of mm-wave frequency range); if the structure is produced using classical CNC technology, it is easier to drill holes than machining the pins (other technologies can be used for production of gap-waveguide components such as sheet metal processing or metallized plastic injection molding). The latter property, the non-dispersive guiding property of the dominant mode, is successfully implemented in the realization of broadband components, such as two-dimensional lenses [44], [46]. The higher-order symmetry principles have recently been used in the development of numerous mm-wave components (example of a Luneburg lens is shown in Fig. 14.), see e.g. [47].

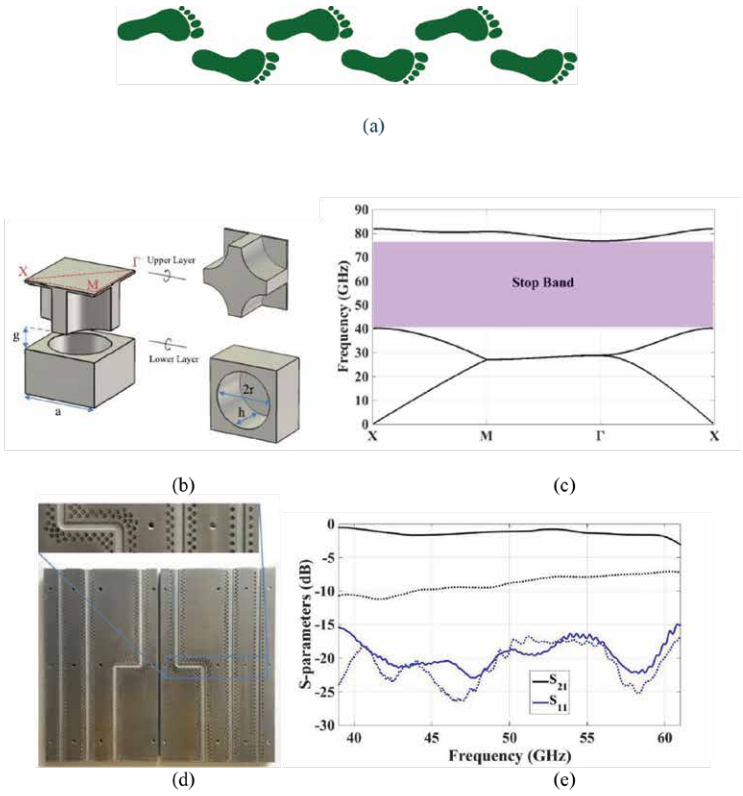

Figure 13. (a) Sketch of glide-symmetric periodic structure; (b) Glide-symmetric holey unit cell; (c) Dispersion diagram of the glide-symmetric holey unit cells; (d) Eperimental prototype of straight and double 90° bent waveguide lines; (e) Comparison of S-parameters corresponding to straight waveguides with and without glide-symmetric holey periodic structure (reprinted from [42]).

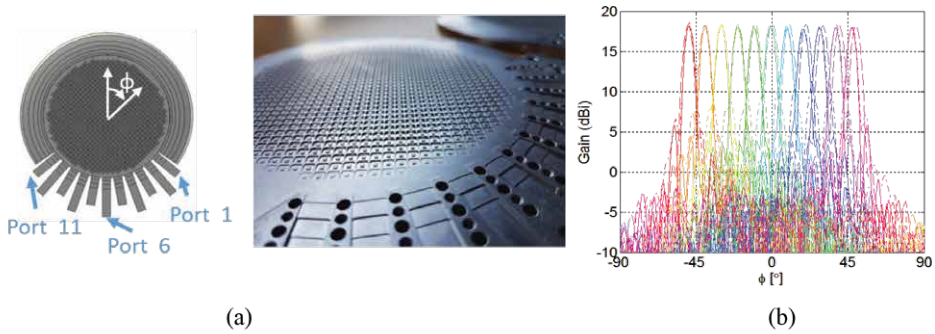

Figure 14. A glide-symmetric Luneburg lens antenna. (a) The manufactured prototype; (b) Simulated and measured radiation patterns at 28 GHz (reprinted from [46]).

4 Metasurfaces

In the early 2000s, metamaterials began to develop intensively – volumetric periodic structures with a period much smaller than the wavelength. The main goal was to develop structures with permeability or permittivity that cannot be found in nature. Thus, materials with negative permittivity/permeability or with structural parameters close to zero were constructed. For many new ideas, proof-of-concept prototypes were created, such as structures with the reversed Snell's law, invisibility cloaks, superluminal lenses, etc. (see e.g. [48], [49]). Split-ring resonators were considered the basic building element for achieving negative permeability, and periodic arrays of parallel wires for negative permittivity [50]. The materials under consideration were often difficult to implement, and many of them had problems with the operating frequency band and losses (one reason being frequent use of resonant structures).

Another origin of metasurfaces is also found in Frequency Selective Surfaces (FSS). The development of FSS was intensive in the last quarter of the 20th century, with the goal to develop surfaces with tailored reflection/transmission properties in terms of frequency and angle of incidence. The elements of FFS are usually designed to have resonant properties, i.e., the typical length of FSS element is around half wavelength. In this way, the FSS based on patches is reflective around the patch-resonant frequency and transmissive otherwise, while the FSS based on slots has opposite properties. Typical applications of FSS are in multi-reflector systems, in which one sub-reflector (realized using FSS) acts as a reflector for one frequency band and is transparent for other frequency band. An overview of FSS can for instance be found in [6], [51], and [52].

Around 2010, metasurfaces began to develop – two-dimensional variants of metamaterials [53] – [55]. The period was still much smaller than the wavelength, however the traditional process of producing printed circuit boards (PCBs) was considered a manufacturing method, and recently, additive manufacturing (the so-called 3D printing) has been explored. Furthermore, resonant structures were not used, which allowed for wider operating frequency bands and lower losses. The first considered application was diffraction surfaces, i.e., printed structures that redirect the propagation direction of EM waves. Metasurfaces that focus EM waves in the near field (2D variant of a superluminal lens) were also considered [56], as well as metasurfaces that represent microwave holograms [57], [58]. These were followed by many other applications, which can roughly be categorized into two groups – metasurfaces that change the direction of propagation, polarization, and other properties of the incident EM wave (the so-called transparent metasurfaces), and metasurfaces that direct and control the scattering of EM waves propagating along the metasurface (the so-called surface wave metasurfaces). Both types of metasurfaces are shown in Figure 15.

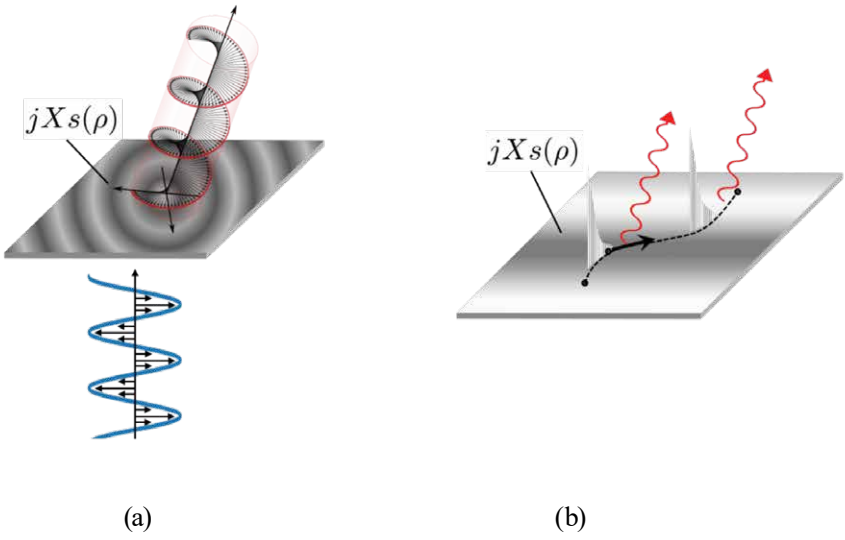

Figure 15. (a) Metasurfaces for plane wave manipulation (both the direction of propagation and polarization of the incident EM wave can be modified); (b) Metasurfaces for surface wave manipulation (the direction of propagation along the surface can be modified and transition to leaky-waves can be obtained).

While metamaterials were described by volumetric parameters – effective permeability and permittivity, metasurfaces are most commonly described by surface parameters – effective surface impedance. Since often both electric and magnetic responses are desirable, i.e., we would like to obtain a metasurface with bianisotropic response, in general we can model the metasurface with a surface polarizability matrix relating the averaged tangential fields to the induced dipole moments per unit area ($\mathbf{p}^s$ and $\mathbf{m}^s$). For the time-harmonic case, the dipole moments can be expressed as a surface current, resulting in the following idealized model of a metasurface:

$$\begin{pmatrix} \mathbf{J}^s \\ \mathbf{M}^s \end{pmatrix} = j\omega \begin{pmatrix} \mathbf{p}^s \\ \mathbf{m}^s \end{pmatrix} = \begin{pmatrix} \overline{\overline{Y}} & \overline{\overline{\chi}} \\ \overline{\overline{\gamma}} & \overline{\overline{Z}} \end{pmatrix} \begin{pmatrix} \mathbf{E}_{\tan}^{ave} \\ \mathbf{H}_{\tan}^{ave} \end{pmatrix} \tag{6}$$

The obtained boundary conditions are called generalized sheet transition conditions (GSTC), and with them we can accurately model thin metasurfaces corresponding to an array of isolated scatterers (the so-called metafilms) [59] – [61]. The surface parameters $\overline{\overline{Y}}, \overline{\overline{Z}}, \overline{\overline{\chi}}$ and $\overline{\overline{\gamma}}$ describe the electric, magnetic and magneto-electric properties of the considered metasurface.

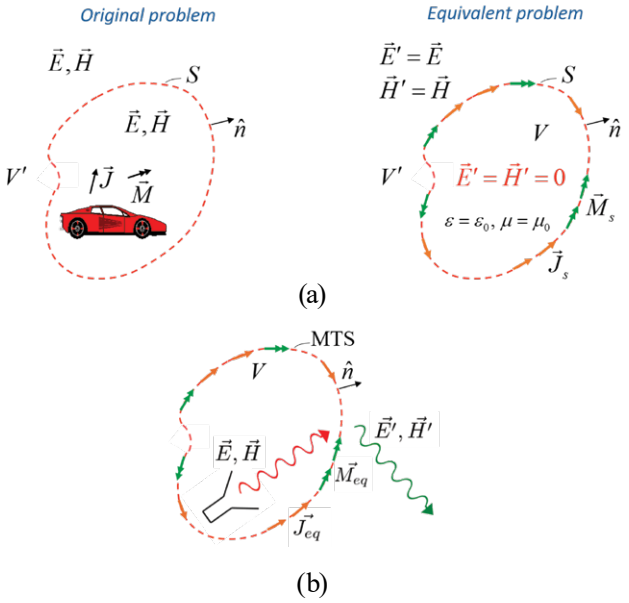

Figure 16. Surface equivalence principle; (a) Mathematical approach in which we define an equivalent problem with the same EM field distribution in the outside region and zero-field distribution in the inside region (Love's theorem), (b) Physical approach in which the metasurface currents achieve the desired EM field distribution in the outside region.

The theoretical framework for transmission metasurfaces (i.e., for metasurface for plane wave manipulation) can be described using the surface equivalence principle [62]. The equivalence principle is a tool for analyzing many EM problems (see Figure 16.a). A complex EM problem is divided into two parts (two volumes); the goal is to obtain a solution to the observed problem in volume 2 without going into details of the EM field distribution in volume 1. Therefore, we define an equivalent problem that is identical to the original problem in volume 2, while in volume 1, we have a different distribution of the EM field – the only condition is that it satisfies Maxwell's equations (often, for simplicity, we assume that the EM field within volume 1 is zero – the so-called Love's equivalence principle). Since, in the equivalent problem, there is generally a discontinuity in the tangential components of the electric and magnetic fields at the boundary between the two volumes, this discontinuity is accounted for using the equivalent magnetic and electric currents:

$$\mathbf{J}_{eq} = \hat{n} \times \left(\mathbf{H}_2 - \mathbf{H}_1 \right), \qquad \mathbf{M}_{eq} = -\hat{n} \times \left(\mathbf{E}_2 - \mathbf{E}_1 \right). \tag{7}$$

A similar principle is used in the approximation of good conductors – perfect electric conductor (PEC) – where the discontinuity in the tangential magnetic field is accounted for by surface currents flowing along the PEC.

Before the emergence of metamaterials, the principle of equivalence was exclusively a theoretical framework for solving EM problems. With the appearance of metasurfaces, the idea to experimentally apply the equivalence principle emerged. Specifically, if we consider a typical problem of transmission metasurfaces (Figure 16.b), we want the EM field distribution in volume 2 not to correspond to the distribution excited by the feeding structure. In other words, in volume 1, we have an excitation distribution of the EM field (excited by the feeding structure), while in volume 2, we would like to have the desired EM field distribution. The natural discontinuity in the EM field distribution will be "covered" by the corresponding metasurface, where the equivalent electric and magnetic currents will correspond to the currents flowing along the considered metasurface. In this way, the principle of equivalence becomes an experimental framework for creating new EM structures [63] – [67].

Metasurfaces obtained to be implemented in this way are often bianisotropic (described by equations (6)); in practice, it is not always clear how to implement this. Fortunately, they can be implemented via multilayer metasurfaces with electric response only (Figure 17). It should be noted that this is still a printed circuit board technology, thus simple to fabricate. The number of layers needed depends on the desired number of degrees of freedom. Typically, we want to choose the amplitude of the transmitted and reflected EM waves, as well as the phase of the transmitted wave (in practice described

by S-parameters). Therefore, we usually have three degrees of freedom related to the structure we are designing. Such a structure can be implemented with a three-layer metasurface with electric response only, or sometimes a four-layer structure is used with an additional degree of freedom to achieve a wider operating frequency band [68] – [72].

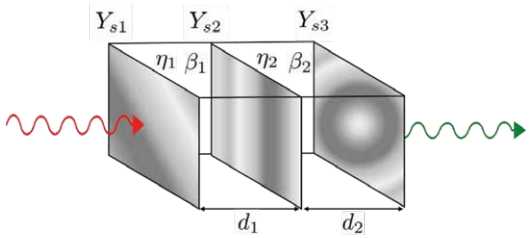

Figure 17. A cascade of three patterned metallic sheets having electrical response only.

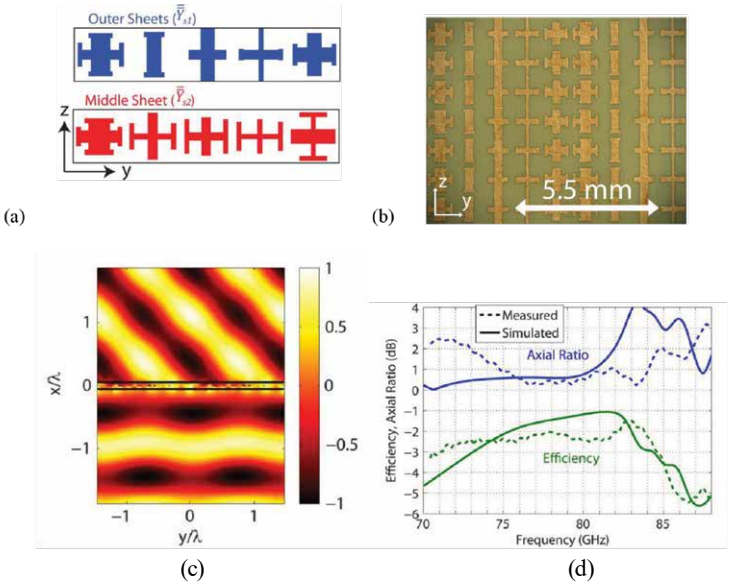

Figure 18. Beam-refracting transmitarray; (a) Geometry of the outer and middle sheets of three-layer realization of the transmitarray, (b) Photography of the transmitarray, (c) Time snapshot of the co-polarized electric field of a incident and transmitted plane wave – the incident wave is linearly polarized, and the transmitted wave is circularly polarized, (d) Efficiency of the beam-refracting transmitarray and the axial ratio of the transmitted field in the direction of the main beam. Figures are reprinted from [64].

As an example of the transmission metasurfaces, let us consider a transmitarray that refracts a normally incident plane wave to an angle 45° and converts the polarization from linear to circular. The working frequency is 77 GHz. The transmitarray is realized as a three-layer metasurface with equal first and third layer. In Figure 18, the unit cell of the outer and middle sheets is given, as well as the photography of the structure. Figure 18 further shows propagation properties of the normal incident EM wave, and the comparison of calculated and measured efficiency and axial ratio of the generated circularly-polarized wave. The details of the structure and the design procedure can be found in [64].

Surface wave metasurfaces can be described in various ways. When it comes to 2D lens antennas, it is natural to consider methods of geometric optics [73]. For example, if we wish to design a 2D lens antenna (placed within the parallel plate waveguide (PPW), similar to previously described design in Fig. 14), the characteristic equation needed for the design process is obtained by the transverse resonance method (here X_s is the surface reactance of metasurface PPW wall, and h_{PPW} is the thickness of the PPW; details can be found in [74], [75]):

$$X_S(k_\rho) = \eta_0 \frac{\alpha_z}{k_0} \tanh(\alpha_z h_{PPW}) . \tag{8}$$

However, we often want to achieve not only the propagation of EM waves along the metasurface, but also the controlled radiation. For this purpose, it is necessary to introduce a perturbation in the surface impedance of the metasurface. This can most easily be considered using the holographic principle.

Gabor first introduced holography as a technique in optics to record a 2D interference pattern of a reference light wave and the light wave reflected from an object [76]. By illuminating the 2D hologram (the recorded interference pattern) with the reference light wave, usually a laser source, it is possible to reconstruct a virtual 3D image of the object [77]. Optical principles can be applied in the microwave region for metasurface design, as Sievenpiper shows in [57], [58], [78]. In optics, ψ_{obj} represents the object wave (beam), while ψ_{ref} represents the reference wave (beam). The interference pattern is then proportional to $\psi_{obj}\psi_{ref}^{*}$. When the hologram is read, i.e., the interference pattern is illuminated by the reference wave, the following term is obtained:

$$\left(\psi_{obj}\psi_{ref}^{*}\right)\psi_{ref} = \psi_{obj}\left|\psi_{ref}\right|^2 , \tag{9}$$

which is a copy of the original object wave. In the metasurface design, ψ_{ref} is substituted with ψ_{surf} , which represents currents generated by the antenna (meta-

surface), and ψ_{obj} is substituted with ψ_{rad} that corresponds to the near field we would like the antenna to radiate. In the simple case, in the case of 1D propagation along metasurface structure in x-direction, ψ_{ref} takes the form of a plane wave:

$$\psi_{surf} = e^{-jk_0 n_{eff} x}, \tag{10}$$

where n_{eff} is the effective refractive index seen by the currents (i.e., effective index of the surface wave mode excited by source), and k_0 is the propagation constant in free space. If the desired radiation pattern of the metasurface is a pencil beam with an elevation angle θ_L, ψ_{rad} takes the form of:

$$\psi_{rad} = e^{-jk_0 x \sin\theta_L}. \tag{11}$$

Then, the surface reactance has the following expression:

$$\begin{aligned} X_s(x) &= X_0\left(1 + M\,\mathrm{Re}\left\{\psi_{rad}\psi_{surf}^{*}\right\}\right) = X_0\left(1 + M\cos\left(k_0\left(n_{eff} - \sin\theta_L\right)x\right)\right) \\ &= X_0\left(1 + M\cos\left(\frac{2\pi}{P_x}x\right)\right) \end{aligned} \tag{12}$$

where X_0 is the average surface reactance, P_x is the period of sinusoidally modulated metasurface, and M is the modulation ratio. In Figure 19, the structure of such modulated surface is shown together with the variation of surface reactance and the obtained radiation pattern. The working frequency of the obtained leaky-wave antenna is f = 20 GHz, the substrate is thick 1.5 mm, and has relative permittivity ε_r = 3.5, the average surface reactance is $X_0 = 0.75\eta_0$, the period of sinusoidally modulated metasurface is P_x = 9.42 mm and the modulation index is M = 0.2. The procedure for determining the geometrical shape of the metasurface is described in [79], and the details about the realized antenna can be found in [80]. The extension to two-dimensional leaky-wave antennas is given in [81] – [83].

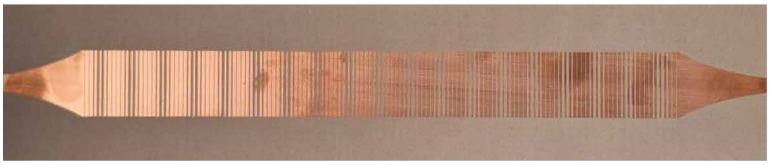

(a)

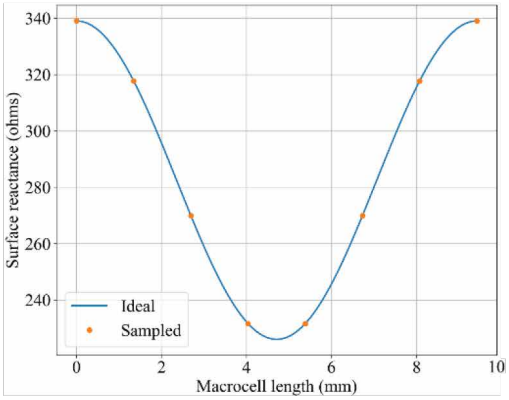

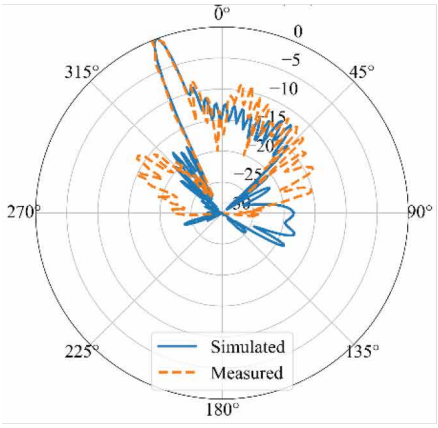

(b) (c)

Figure 19. One-dimensional metasurface leaky-wave antenna; (a) Picture of the antenna, (b) Values of surface reactance used in the design (the full line are the values obtained using holographic approach; the dots represent the sampled values used in practical realization), (c) Calculated and measured radiation pattern.

Conclusion

The paper gives an overview of the theoretical background and the concepts that have led to the development of surface electromagnetics – a broad spectrum of EM surfaces, from canonical uniform surfaces to complex metasurface structures. Practice has shown that almost all innovative and successful designs of EM structures originate from a clear picture of the physical phenomena that was used for the operation of the studied structure. Therefore, the aim of this article is to identify and convey the ideas that have

led to the introduction of certain EM surfaces widely used today. It has been demonstrated through several examples how these concepts can be applied in the development of novel structures that are of particular interest for demanding industrial applications. Finally, this overview covered passive EM surfaces. Recently, however, significant research focus has shifted to tunable and time-varying metasurfaces, which offer a new set of possibilities not covered in this review article.

References

[1] H. Lamb, "On the reflection and transmission of electric waves by a metallic grating," *Proc. Lond. Math. Soc.* vol. s1-29, no. 1, pp. 523-546, 1897.

[2] G. Marconi, C. Franklin, *Reflector for use in wireless telegraphy and telephony*, US Patent 1,301,473, 1919.

[3] R. W. Wood, "Phase-Reversal Zone Plates and Diffraction-Telescopes," *Phil. Mag.,* vol. 45, no. 277, pp. 5ll-523, June 1898.

[4] L. V. Buskirk LV, C. Hendrix, "The zone plate as a radio-frequency focusing element," *IRE Trans. Antennas Propag.* Vol. 9, pp. 319–320, 1961.

[5] A. Oliner and A. Hessel, "Guided waves on sinusoidally-modulated reactance surfaces," *IRE Transactions on Antennas and Propagation*, vol. 7, no. 5, pp. 201-208, Dec. 1959.

[6] B. A. Munk, *Frequency Selective Surfaces: Theory and Design*, Wiley-Interscience, 2000.

[7] F. Yang and Y. Rahmat-Samii, *Electromagnetic Band Gap Structures in Antenna Engineering,* Cambridge University Pres, 2009.

[8] S. Maci, "Electromagnetic Metamaterials and Metasurfaces: A historical journey," *IEEE Antennas and Propagation Magazine*, vol. 66, no. 3, pp. 84-101, June 2024.

[9] P.-S. Kildal, A. A. Kishk and S. Maci, "Special Issue on Artificial Magnetic Conductors, Soft/Hard Surfaces, and Other Complex Surfaces," *IEEE Trans. Antennas Propag.,* vol. 53, no. 1, pp. 2-7, Jan. 2005.

[10] P.-S. Kildal, "Definition of artificially soft and hard surfaces for electromagnetic waves," *Electronics Letters*, vol. 24, no. 3, pp. 168–170, 1988.

[11] P.-S. Kildal, "Artificially soft and hard surfaces in electromagnetics and their application to antenna design," *IEEE Trans. Antennas Propag.,* vol. 38, no. 10, pp. 1537–1544, 1990.

[12] Z. Sipus, H. Merkel, P.-S. Kildal, "Green's functions for planar soft and hard surfaces derived by asymptotic boundary conditions," *IEE Proc. - Microwave Antennas Propag.*, Vol. 144, pp. 321-328, Oct. 1997.

[13] P. S. Kildal and A. A. Kishk, "EM modeling of surfaces with STOP or GO characteristics – artificial magnetic conductors and soft and hard surfaces," *Applied Computational Electromagnetics Society Journal*, vol. 18, pp. 31–40, 2003.

[14] E. Rajo-Iglesias, M. Caiazzo, L. Inclán-Sánchez, P.-S. Kildal, "Comparison of bandgaps of mushroom-type EBG surface and corrugated and strip-type soft surfaces," *IET Microw. Antennas Propag.*, Vol. 1, pp. 184 – 189, 2007.

[15] E. Rajo-Iglesias, "Designing the surfaces (EBG, soft surfaces, parallel-plate stopbands)," Lecture notes, PhD course *Artificial EBG surfaces and metamaterials for antennas,* Chalmers University of Technology, Gothenburg, Sweden, October 26-30, 2009.

[16] Z. Ying, P.-S. Kildal and A. A. Kishk, "Study of different realizations and calculation models for soft surfaces by using a vertical monopole on a soft disk as a test bed," *IEEE Trans. Antennas Propag.,* vol. 44, no. 11, pp. 1474-1481, Nov. 1996.

[17] Z. Ying and P.-S. Kildal, "Improvements of dipole, helix, spiral, microstrip patch and aperture antennas with ground planes by using corrugated soft surfaces," *IEE Proc. - Microwave Antennas Propag.*, Vol. 143, pp. 244-248, June 1996.

[18] D. Sievenpiper, R. Broas, N. Alexopolous, and E. Yablonovitch, "High impedance electromagnetic surfaces with a forbidden frequency band," *IEEE Trans. Microw. Theory Tech.,* vol. 47, no. 11, pp. 2059–2074, 1999.

[19] G. Tsandoulas and W. Fitzgerald, "Aperture efficiency enhancement in dielectrically loaded horns," *IEEE Trans. Antennas Propag.*vol. 20, no. 1, pp. 69-74, Jan. 1972.

[20] E. Lier and P.-S. Kildal, "Soft and hard horn antennas," *IEEE Transactions on Antennas and Propagation*, vol. 36, no. 8, pp. 1152-1157, Aug. 1988.

[21] E. Lier, "Review of Soft and Hard Horn Antennas, Including Metamaterial-Based Hybrid-Mode Horns," *IEEE Antennas and Propagation Magazine*, vol. 52, no. 2, pp. 31-39, April 2010.

[22] P.-S. Kildal, "Hard horns," Lecture notes, PhD course *Artificial EBG surfaces and metamaterials for antennas,* Chalmers University of Technology, Gothenburg, Sweden, October 26-30, 2009.

[23] F. Yang and Y. Rahmat-Samii, "A low profile circularly polarized curl antenna over electromagnetic band-gap (EBG) surface," *Microwave Optical Tech. Lett.,* vol. 31, no. 3, 165–8, 2001.

[24] F. Yang and Y. Rahmat-Samii, "Microstrip antennas integrated with electromagnetic band-gap (EBG) structures: a low mutual coupling design for array applications*," IEEE Trans. Antennas Propagat.,* vol. 51, no. 10, 2936–46, 2003.

[25] C. H. Walter, *Traveling Wave Antennas*, Dover Publications, 1970.

[26] P.-S. Kildal, E. Alfonso, A. Valero-Nogueira, and E. Rajo-Iglesias, "Local Metamaterial-Based Waveguides in Gaps Between Parallel Metal Plates," *IEEE Antennas and Wireless Propagation Letters*, vol. 8, 2009, pp. 84–87.

[27] P.-S. Kildal, A. Zaman, E. Rajo-Iglesias, E. Alfonso, and A. Valero-Nogueira, "Design and Experimental Verification of Ridge Gap Waveguide in Bed of Nails for Parallel-Plate Mode Suppression," *IET Microwaves, Antennas & Propagation*, vol. 5, no. 3, Feb. 21 2011, pp. 262–70.

[28] A. Valero-Nogueira, E. Alfonso, J. I. Herranz and P. -S. Kildal, "Experimental Demonstration of Local Quasi-TEM Gap Modes in Single-Hard-Wall Waveguides," *IEEE Microwave and Wireless Components Letters*, vol. 19, no. 9, pp. 536-538, Sept. 2009.

[29] A. Valero-Nogueira, E. Alfonso, J. Herranz, and M. Baquero, "Planar slot-array antenna fed by an oversized quasi-TEM waveguide," *Microwave and Optical Technology Letters*, vol. 49, no. 8, pp. 1875–1877, 2007.

[30] E. Rajo-Iglesias, M. Ferrando-Rocher and A. U. Zaman, "Gap Waveguide Technology for Millimeter-Wave Antenna Systems," in *IEEE Communications Magazine*, vol. 56, no. 7, pp. 14-20, July 2018.

[31] D. Zarifi, A. Farahbakhsh, A. U. Zaman, and P. S. Kildal, "Design and fabrication of a high gain 60-GHz corrugated slot antenna array with ridge gap waveguide distribution layer," *IEEE Transactions on Antennas and Propagation*, vol. 64, pp. 2905–2913, 2016.

[32] A. Farahbakhsh, D. Zarifi, and A. U. Zaman, "60-GHz groove gap waveguide based wideband H-plane power dividers and transitions: For use in high-gain slot array antenna," *IEEE Transactions on Microwave Theory and Techniques*, vol. 65, pp. 4111–4121, 2017.

[33] J. Liu, A. Vosoogh, A. U. Zaman and J. Yang, "Design and Fabrication of a High-Gain 60-GHz Cavity-Backed Slot Antenna Array Fed by Inverted Microstrip Gap Waveguide", *IEEE Transactions on Antennas and Propagation*, vol. 65, no. 4, pp. 2117-2122, April 2017.

[34] Jiménez Sáez, A. Valero-Nogueira, J. I. Herranz and B. Bernardo, "Single-Layer Cavity-Backed Slot Array Fed by Groove Gap Waveguide," *IEEE Antennas and Wireless Propagation Letters*, vol. 15, no. , pp. 1402-1405, 2016.

[35] E. Alfonso, S. Carlred, S. Carlsson, L.-I. Sjöqvist, "Contactless Flange Adapters for Mm-Wave Measurements," *2017 11th European Conference on Antennas and Propagation (EUCAP)*, Paris, France, 2017, pp. 1690-1693.

[36] E. Rajo-Iglesias, A. U. Zaman, and P. S. Kildal, "Parallel plate cavity mode suppression in microstrip circuit packages using a lid of nails," *IEEE Microwave and Wireless Components Letters*, vol. 20, pp. 31–33, 2010.

[37] A. A. Brazalez, A. U. Zaman, and P. S. Kildal, "Improved microstrip filters using PMC packaging by lid of nails," *IEEE Transactions on Components, Packaging and Manufacturing Technology*, vol. 2, pp. 1075–1084, 2012.

[38] A. U. Zaman, M. Alexanderson, T. Vukusic and P. -S. Kildal, "Gap Waveguide PMC Packaging for Improved Isolation of Circuit Components in High-Frequency Microwave Modules," *IEEE Transactions on Components, Packaging and Manufacturing Technology*, vol. 4, no. 1, pp. 16-25, Jan. 2014.

[39] M. Vukomanovic, J. -L. Vazquez-Roy, O. Quevedo-Teruel, E. Rajo-Iglesias and Z. Sipus, "Gap Waveguide Leaky-Wave Antenna," in *IEEE Transactions on Antennas and Propagation*, vol. 64, no. 5, pp. 2055-2060, May 2016.

[40] P. J. Crepeau and P. R. McIsaac, "Consequences of symmetry in periodic structures," *Proc. IEEE*, vol. 52, no. 1, pp. 33–43, Jan. 1964.

[41] A. Hessel, M. H. Chen, R. C. M. Li, and A. A. Oliner, "Propagation in periodically loaded waveguides with higher symmetries," Proc. IEEE, vol. 61, no. 2, pp. 183–195, Feb. 1973.

[42] M. Ebrahimpouri, E. Rajo-Iglesias, Z. Sipus and O. Quevedo-Teruel, "Cost-Effective Gap Waveguide Technology Based on Glide-Symmetric Holey EBG Structures," in *IEEE Transactions on Microwave Theory and Techniques*, vol. 66, no. 2, pp. 927-934, Feb. 2018.

[43] Q. Chen, F. Mesa, X. Yin and O. Quevedo-Teruel, "Accurate Characterization and Design Guidelines of Glide-Symmetric Holey EBG," *IEEE Transactions on Microwave Theory and Techniques*, vol. 68, no. 12, pp. 4984-4994, Dec. 2020.

[44] O. Quevedo-Teruel, M. Ebrahimpouri, and M. N. M. Kehn, "Ultrawideband metasurface lenses based on off-shifted opposite layers," *IEEE Antennas Wireless Propag. Lett.,* vol. 15, pp. 484–487, Dec. 2016.

[45] O. Dahlberg, R. C. Mitchell-Thomas, O. Quevedo-Teruel1, "Reducing the dispersion of periodic structures with twist and polar glide symmetries," *Sci. Reports, vol.* 7, 2017.

[46] O. Quevedo-Teruel, J. Miao, M. Mattsson, A. Algaba-Brazalez, M. Johansson, and L. Manholm, "Glide-symmetric fully metallic Luneburg lens for 5G communications at Ka-band," *IEEE Antennas Wireless Propag. Lett.,* vol. 17, no. 9, pp. 1588–1592, Sept. 2018.

[47] O. Quevedo-Teruel, G. Valerio, Z. Sipus and E. Rajo-Iglesias, "Periodic Structures With Higher Symmetries: Their Applications in Electromagnetic Devices," *IEEE Microwave Magazine*, vol. 21, no. 11, pp. 36-49, Nov. 2020.

[48] N. Engheta and R. Ziolkowski (Eds.)*, Metamaterials: Physics and Engineering Explorations.* Wiley-IEEE Press, 2006.

[49] W. Douglas and K. Do-Hoon (Eds.), *Transformation Electromagnetics and Metamaterials*, Springer, 2013.

[50] D. Smith, W. Padilla, D. Vier, S. Nemat-Nasser, and S. Schultz, "Composite medium with simultaneously negative permeability and permittivity," *Phys. Rev. Lett.,* vol. 84, no. 18, pp. 4184–4187, 2000.

[51] R. Mittra, C. H. Chan and T. Cwik, "Techniques for analyzing frequency selective surfaces-a review," *Proceedings of the IEEE*, vol. 76, no. 12, pp. 1593-1615, Dec. 1988.

[52] J. C. Vardaxoglou, *Frequency Selective Surface: Analysis and Design*, Research Studies Pre, 1996.

[53] C. Pfeiffer and A. Grbic, "A printed, broadband Luneburg lens antenna," *IEEE Trans. on Antennas and Propagation*, vol. 58, no. 9, pp. 3055 – 3059, Sept. 2010.

[54] N. Yu, P. Genevet, M. Kats, F. Aieta, J. Tetienne, F. Capasso, and Z. Gaburro, "Light propagation with phase discontinuities: generalized laws of reflection and refraction," *Science*, vol. 334, pp. 333-3337, Oct. 2011.

[55] C. L. Holloway, E. F. Kuester, J. A. Gordon, J. O'Hara, J. Booth, and D. R. Smith, "An overview of the theory and applications of metasurfaces: the two-dimensional equivalents of metamaterials," IEEE Antennas and Propagation Magazine, vol. 54, pp. 10-35, Apr. 2012.

[56] A. Grbic and R. Merlin, "Near-field focusing plates and their design," *IEEE Trans. Antennas Propag.*, vol. 56, no. 10, pp. 3159–3165, Oct. 2008.

[57] D. Sievenpiper, J. Colburn, B. Fong, J. Ottusch and J. Visher, "Holographic artificial impedance surfaces for conformal antennas," *2005 IEEE Antennas and Propagation Society International Symposium*, Washington, DC, USA, 2005, pp. 256-259.

[58] B. H. Fong, J. S. Colburn, P. R. Herz, J. J. Ottusch, D. F. Sievenpiper and J. L. Visher, "Polarization controlling holographic artificial impedance surfaces," *2007 IEEE Antennas and Propagation Society International Symposium*, Honolulu, HI, USA, 2007, pp. 3824-3827.

[59] E. Kuester, M. Mohamed, M. Piket-May, C. Holloway, "Averaged Transition Conditions for Electromagnetic Fields at a Metafilm", *IEEE Trans. Antennas Propag,* vol. 51, No. 10, pp. 2641–2651, Oct. 2003.

[60] F. Yang and Y. Rahmat-Samii (Eds.), *Surface Electromagnetics: With Applications in Antenna, Microwave, and Optical Engineering*, Cambridge University Press, 2019.

[61] A. Ghaneizadeh and M. Joodaki, "Generalized Sheet Transition Conditions (GSTCs) in Electromagnetic Metasurface Modeling," *IEEE Access*, vol. 12, pp. 74305-74326, 2024.
[62] C. A. Balanis, *Advanced Electromagnetic Engineering,* John Wiley & Sons, 2011.
[63] C. Pfeiffer and A. Grbic, "Metamaterial Huygens' surfaces: Tailoring wave fronts with reflectionless sheets," *Phys. Rev. Lett*., vol. 110, no. 19, p. 197,401, May 2013.
[64] C. Pfeiffer and A. Grbic, "Millimeter-wave transmitarrays for wavefront and polarization control," *IEEE Trans. Microw. Theory Techn*., vol. 61, no. 12, pp. 4407–4417, Dec. 2013.
[65] M. Selvanayagam and G. V. Eleftheriades, "Discontinuous electromagnetic fields using orthogonal electric and magnetic currents for wavefront manipulation," *Opt. Express*, vol. 21, no. 12, p. 14,409, 2013.
[66] J. P. Wong, M. Selvanayagam, and G. V. Eleftheriades, "Design of unit cells and demonstration of methods for synthesizing Huygens metasurfaces," *Photon. Nanostruct. – Fundam. Appl*., vol. 12, no. 4, pp. 360–375, Jul. 2014.
[67] K. Achouri, M. A. Salem, and C. Caloz, "General metasurface synthesis based on susceptibility tensors," *IEEE Trans. Antennas Propag.*, vol. 63, no. 7, pp. 2977–2991, Jul. 2015.
[68] C. Pfeiffer and A. Grbic, "Bianisotropic metasurfaces for optimal polarization control: Analysis and synthesis," *Phys. Rev. Appl*., vol. 2, p. 044011, Oct. 2014.
[69] J. P. S. Wong, A. Epstein and G. V. Eleftheriades, "Reflectionless Wide-Angle Refracting Metasurfaces," in *IEEE Antennas and Wireless Propagation Letters*, vol. 15, pp. 1293-1296, 2016.
[70] A. Epstein and G. V. Eleftheriades, "Arbitrary power-conserving field transformations with passive lossless omega-type bianisotropic metasurfaces," *IEEE Trans. Antennas Propag.*, vol. 64, no. 9, pp. 3880–3895, Sep. 2016.
[71] L. Szymanski, B. O. Raeker, C. -W. Lin, and A. Grbic, "Fundamentals of lossless, reciprocal bianisotropic metasurface design," *Photonics*, vol. 8, no. 6, pp. 197-218, Jun 2021.
[72] J. Budhu and A. Grbic, "Recent advances in bianisotropic boundary conditions: Theory, capabilities, realizations, and applications," *Nanophotonics*, vol. 10, no. 16, pp. 4075–4112, 2021.
[73] E. Martini, M. Mencagli, D. González-Ovejero, and S. Maci, "Flat optics for surface waves," *IEEE Trans. Antennas Propag.*, vol. 64, no. 1, pp. 155–166, Jan. 2016.
[74] M. Bosiljevac, M. Casaletti, F. Caminita, Z. Sipus, S. Maci, "Non-uniform Metasurface Luneburg Lens Antenna Design," *IEEE Trans. Antennas Propag,* vol. 60, pp. 4065-4073, Sep. 2012.

[75] S. Maci, G. Minatti, M. Casaletti, and M. Bosiljevac, "Metasurfing: Addressing waves on impenetrable metasurfaces," *IEEE Antennas Wireless Propag. Lett*., vol. 10, pp. 1499–1502, 2011.

[76] D. Gabor. A new microscopic principle. *Nature*, vol. 161(4098), pp. 777–778, May 1948.

[77] P Hariharan. *Cambridge studies in modern optics: Optical holography: Principles, techniques and applications*, Cambridge University Press, Cambridge, England, 2 edition, June 2012.

[78] Bryan H. Fong, Joseph S. Colburn, John J. Ottusch, John L. Visher, and Daniel F. Sievenpiper. "Scalar and tensor holographic artificial impedance surfaces," *IEEE Trans. Antennas Propag,* vol. 58, pp. 3212–3221, Oct. 2010.

[79] A. M. Patel and A. Grbic, "A printed leaky wave antenna based on a sinusoidally-modulated reactance surface," *IEEE Trans. Antennas Propag.*, vol. 59, no. 6, pp. 2087–2096, Jun. 2011.

[80] D. Mikulić, „Analysis and synthesis of space modulated metasurfaces for leaky wave radiation," University of Zagreb, Faculty of Electrical Engineering and Computing, Internal report, 2024.

[81] G. Minatti *et al*., "Modulated metasurface antennas for space: Synthesis, analysis and realizations," *IEEE Trans. Antennas Propag.*, vol. 63, no. 4, pp. 1288–1300, Apr. 2015.

[82] G. Minatti, F. Caminita, E. Martini, and S. Maci, "Flat optics for leaky-waves on modulated metasurfaces: Adiabatic Floquet-wave analysis," *IEEE Trans. Antennas Propag.*, vol. 64, no. 9, pp. 3896–3906, Sep. 2016.

[83] G. Minatti, F. Caminita, E. Martini, M. Sabbadini, and S. Maci, "Synthesis of modulated-metasurface antennas with amplitude, phase, and polarization control," *IEEE Trans. Antennas Propag*, vol. 64, no. 9, pp. 3907–3919, Sep. 2016.

POVRŠINSKI ELEKTROMAGNETIZAM: RAZVOJ, MODELIRANJE I PRIMJENE

Sažetak

Idealni rubni uvjeti široko su prihvaćeni u većini elektromagnetskih računalnih programa za aproksimaciju stvarnih površina ili materijala. Na primjer, uobičajeno je zamijeniti metalne vodiče sa savršenim električnim vodičem, čime se značajno smanjuje potreba za računalnim resursima. Iako magnetski vodiči na mikrovalnim frekvencijama ne postoje u prirodi, rubni uvjet za savršeni magnetski vodič također se često koristi u prvoj fazi elektromagnetskog dizajna. Razlog tome je što neke umjetne površine pokazuju svojstva savršenog magnetskog vodiča u određenim frekvencijskim pojasevima. Također, osim gore spomenutih, tijekom posljednjih godina pojavile su se i mnoge druge vrste umjetnih površina, koje se koriste u raznim primjenama. Ovaj rad daje pregled površinskog elektromagnetizma, pojma koji se odnosi na širok spektar elektromagnetskih površina, počevši od najjednostavnijih kanonskih uniformnih površina do složenih metapovršinskih struktura. Pritom se razmatra razvoj i primjene kanonskih elektromagnetskih površina za mikrovalne primjene, pokazujući njihovu sposobnost poboljšanja svojstava vođenja i zračenja elektromagnetskih valova. To uključuje upravljanje elektromagnetskom spregom između različitih dijelova razmatranih komponenata te kontrolu svojstava zračenja antena poput smjera zračenja, širine glavne latice, razine bočnih latica i polarizacije. Rad također predstavlja teoretske modele koji se mogu koristiti u početnoj fazi dizajna u kojoj se razmatrana struktura modelira pomoću kanonskih elektromagnetskih površina. Površinski elektromagnetizam pokazao se kao svestrano, robusno i isplativo rješenje za dizajn nove generacije elektromagnetskih komponenata, omogućujući potpunu prilagodbu željenih svojstava komponenti.

Zvonimir Šipuš
University of Zagreb
Faculty of Electrical Engineering and Computing
Unska 3, 10000 Zagreb Croatia
e-mail: zvonimir.sipus@fer.unizg.hr

Marko Bosiljevac
University of Zagreb
Faculty of Electrical Engineering and Computing
Unska 3, 10000 Zagreb Croatia
e-mail: marko.bosiljevac@fer.unizg.hr

Davorin Mikulić
University of Zagreb
Faculty of Electrical Engineering and Computing
Unska 3, 10000 Zagreb Croatia
e-mail: davorin.mikulic@fer.unizg.hr